

Contribution of classical correlation and entanglement in the non-classical teleportation fidelity

Priyanka Chowdhury^{1, *}

¹*Department of Physics, Basirhat College, Basirhat, 743412, India*

It is well known that entanglement is the resource of quantum teleportation. Teleportation can be accomplished using classical correlation (CC) with a teleportation fidelity (TF) upto $2/3$. In the present work we have studied TF, entanglement and CC in the presence of decoherence. We have found that significant increment of CC with respect to the strength of decoherence can lead TF in the non-classical region while entanglement is decreasing. We have also studied the protection of TF and entanglement using the technique of weak measurement and reverse weak measurement (WMRWM). Here we found that maximum protection of entanglement does not optimize the TF and CC. While optimization of TF indicates maximization of CC. Therefore, both entanglement and classical correlation of the shared state take part in the teleportation in a complex manner that needs to be explored in the future.

I. INTRODUCTION

Nonlocal quantum correlation forms the fundamental resource of different information processing tasks [1]. For example, entanglement [2] is the fundamental resource of quantum teleportation [3–7], where the unknown state of a quantum system has been transferred at a distant location with the help of local operation and communication of 2 classical bits without sending the system. Interestingly, The efficiency of teleportation, i.e., the fidelity of the teleported state with respect to the given unknown state can be achieved (on average) upto $2/3$ with the help of shared classical correlation [8, 9]. Shared nonlocal quantum correlation, e.g., entanglement is necessary to achieve teleportation fidelity in the non-classical region, i.e., greater than $2/3$. The teleportation fidelity (TF) takes the maximum value of 1 for the shared maximally entangled state.

The maximum TF obtained using an entangled state can be quantified by its fully entangled fraction (FEF) [10], and it is also a function of concurrence [14], a measure of entanglement [15–18]. The TF becomes non-classical when concurrence is non-vanishing, and FEF is larger than $1/2$. TF increases (decreases) with larger (smaller) values of concurrence and FEF. For example, in the presence of decoherence, the entanglement decreases gradually with the strength of the decoherence parameter [21, 40–43]. As a result, TF also decreases over the strength of decoherence [25–27]. Note that under certain circumstances, entanglement can be generated or increased when the associated systems collectively interact with a common environment [28–30]. Similarly, decoherence can enhance the TF from classical region to non-classical region [11, 31] without increasing entanglement.

There are many techniques of protecting quantum correlation in the presence of decoherence [24, 27–30, 32–39]. For example, environmental interaction modeled

by the amplitude damping channel (ADC) can be suppressed by the technique of weak measurement and reverse weak measurement (WMRWM) [27, 32–35]. It has been theoretically and experimentally verified that coherence [33, 34], entanglement [35], teleportation [27] can be protected in the presence of ADC. Note that WMRWM does not create entanglement if entanglement sudden death (ESD) [40–43] occurs.

When ESD occurs, the bipartite state is not useful for information processing tasks. But, if entanglement becomes non-zero, the state at least can be used for teleportation. Now, due to the effect of decoherence, if the state is still entangled, does the state also useful for teleportation? Using the WMRWM technique, entanglement can be increased by increasing the strength of weak measurement. Therefore, does the optimized protection of entanglement using WMRWM imply optimized protection of TF? In this work, we have addressed the above questions. For this purpose, two qubits have been prepared in the maximally entangled state, and they are allowed to interact with the environment via ADC. Decoherence can activate TF from the classical to the non-classical region or deactivate it from the non-classical to the classical region. We find that the activation of TF is due to the significant enhancement of CC with respect to the strength of decoherence while entanglement reduces gradually. Although the technique of WMRWM is used to minimize the effect of ADC, we have shown that the optimized protection of TF does not always imply optimization of entanglement. In this case, CC plays a significant role in maximizing TF. This study opens the a new perspective on TF, entanglement and CC.

II. MEASURE OF ENTANGLEMENT, TF AND CLASSICAL CORRELATION

It has already been proved that for realizing the non-classical teleportation fidelity, the entanglement of the shared state should be non-zero [8, 9, 17, 44]. The entanglement of a given two-qubit state ρ_{AB} can be quantified

* priyanka.chowdhury@basirhatcollege.org

by the concurrence [14]. The concurrence of the state ρ_{AB} is defined by [14]

$$\mathcal{C}(\rho_{AB}) = \max \left[0, \sqrt{\lambda_1} - \sqrt{\lambda_2} - \sqrt{\lambda_3} - \sqrt{\lambda_4} \right], \quad (1)$$

where λ_i 's are eigenvalues of the matrix $\rho_{AB}\tilde{\rho}_{AB}$ in descending order. Here, $\tilde{\rho}_{AB} = (\sigma_y \otimes \sigma_y)\rho_{AB}^*(\sigma_y \otimes \sigma_y)$, where the superscript “*” represents the complex conjugate. The value of \mathcal{C} is bounded by $[0, 1]$, where the lower bound 0 and upper bound 1 correspond to separable states and maximally entangled states, respectively.

How efficiently one can perform teleportation is quantified by the TF, which is the fidelity of the teleported state with the given unknown state. The maximum attainable TF of the shared entangled state ρ_{AB} is given by [10]

$$F(\rho_{AB}) = \frac{2f(\rho_{AB}) + 1}{3}. \quad (2)$$

Here, $f(\rho_{AB})$ is the FEF calculated as [45]

$$f(\rho_{AB}) = \max_{|\phi\rangle \in \text{MES}} \langle \phi | \rho_{AB} | \phi \rangle, \quad (3)$$

where the maximum is taken over all possible maximally entangled state (MES). The state ρ_{AB} is said to be useful for teleportation, i.e., $F(\rho_{AB}) > 2/3$ when $f(\rho_{AB}) > 1/2$.

In the Ref. [11], the author concluded that the classical correlation (CC) of the shared state ρ_{AB} sometimes plays a significant role in obtaining non-classical TF. The maximum classical correlation can be obtained from the total correlation of the shared state [12, 13]. The total correlation of the state ρ_{AB} is given by $\mathcal{I}(\rho_{AB}) = \mathcal{S}(\rho_A) + \mathcal{S}(\rho_B) - \mathcal{S}(\rho_{AB})$, where $\mathcal{S}(\rho_i)$ is the von-Neumann entropy of the state ρ_i with $i \in \{A, B, AB\}$. CC is calculated by measuring one of the systems, say, the system B with the projectors $\{\Pi_j^B\}$, where j corresponds to different measurement outcomes. The classical correlation can be written as [12, 13]

$$CC_B(\rho_{AB}) = \max_{\Pi_j^B} \left[\mathcal{S}(\rho_A) - \sum_j p_j^{\Pi_j^B} \mathcal{S}(\rho_{A|j}^{\Pi_j^B}) \right], \quad (4)$$

where the maximum is taken over all possible sets of orthogonal projectors $\{\Pi_j^B\}$ on the system B . $CC_B(\rho_{AB})$ attains the maximum value “1” for the maximally entangled states.

III. ENVIRONMENTAL INTERACTION MODELLED BY ADC

For the purpose of teleportation, the sender, say, Alice prepares two-qubit in a maximally entangled state

$$|\psi\rangle_{12} = \frac{|00\rangle_{12} + |11\rangle_{12}}{\sqrt{2}}, \quad (5)$$

where the subscript $i \in \{1, 2\}$ corresponds to the i th qubit. Alice sends 2nd qubit to the receiver, say, Bob separated at a distant location. Note that both concurrence

and TF take the maximum value, unity for the prepared state $|\psi\rangle_{12}$. When the 2nd qubit transits through the environment, it interacts with the environment. Due to the effect of the environmental interaction, the initially prepared pure entangled state becomes a mixed entangled state. As a result, the entanglement between two-qubit decreases and the TF drops. When the TF falls below $2/3$, the state becomes useless for teleportation. In this work, we consider two different scenarios. In the 1st scenario, one of the qubits, say, 2nd qubit interacts with the environment, and in the second scenario, both qubits interact with the environment.

There are many theoretical models of environmental interaction with quantum systems [1]. For the purpose of the present work, the environmental interaction modelled by ADC has been considered. According to this model, when the i th qubit is in the state $|0\rangle_i$ (ground energy state), it does not interact with the environment. When the qubit is in the state $|1\rangle_i$ (excited energy state), the qubit jumps to the state $|0\rangle_i$ with the probability D_i by spontaneously emitting a photon, and it remains unaffected with probability $\bar{D}_i = 1 - D_i$. The interaction can be written as

$$\begin{aligned} |0\rangle_i |0\rangle_E &\longrightarrow |0\rangle_i |0\rangle_E, \\ |1\rangle_i |0\rangle_E &\longrightarrow \sqrt{\bar{D}_i} |1\rangle_i |0\rangle_E + \sqrt{D_i} |0\rangle_i |1\rangle_E, \end{aligned} \quad (6)$$

where $|0\rangle_E$ is the initial state of the environment, and $i \in \{1, 2\}$. Here, D_i is the strength of interaction between i th qubit and the environment.

The effect of ADC on the i th ($i \in \{1, 2\}$) qubit in the state ρ_i ($\rho_{1(2)} = \text{Tr}_{2,(1)}[\rho_{12}]$) can be expressed as the map Λ ,

$$\Lambda(\rho_i) = W_{i,0} \rho_i W_{i,0}^\dagger + W_{i,1} \rho_i W_{i,1}^\dagger, \quad (7)$$

where the Kraus operators $W_{i,j}$ are given by

$$\begin{aligned} W_{i,0} &= \begin{pmatrix} 1 & 0 \\ 0 & \sqrt{\bar{D}_i} \end{pmatrix}, \\ W_{i,1} &= \begin{pmatrix} 0 & \sqrt{D_i} \\ 0 & 0 \end{pmatrix}, \end{aligned} \quad (8)$$

and $\sum_{j=0}^1 W_{i,j} W_{i,j}^\dagger = \text{I}$.

IV. VARIATION OF ENTANGLEMENT, CLASSICAL CORRELATION AND TF WITH RESPECT TO DECOHERENCE MODELLED BY ADC

To study the effect of ADC on entanglement and TF, let us consider two different scenarios, i.e., “Scenario - I” and “Scenario - II”. In the “Scenario - I” and “Scenario - II”, one of the qubit, say, 2nd qubit and both qubits are affected by the environment, respectively. The TF, concurrence and CC have been compared in the both scenarios.

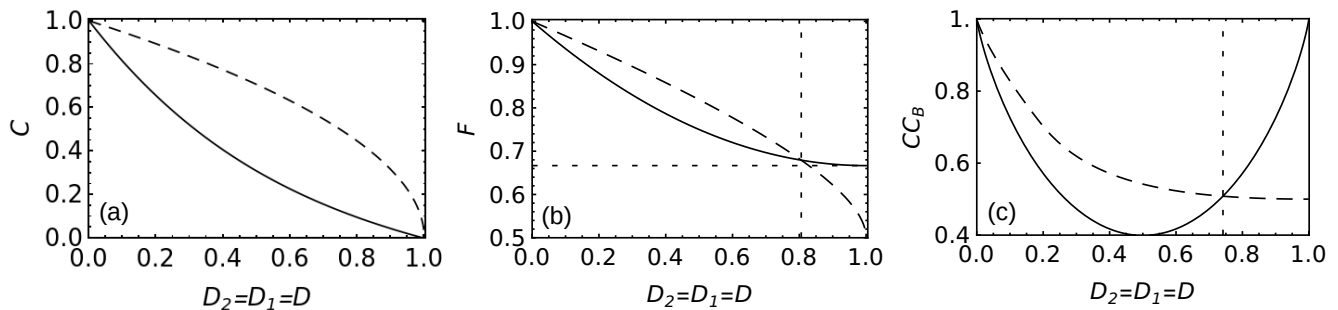


FIG. 1. Variation of (a) entanglement, (b) teleportation fidelity and (c) classical correlation of the state ρ_{12}^D (of Eq. 9) and ρ_{12}^{DD} (of Eq. 11) with respect to strength of decoherence $D_2 = D_1 = D$. Dashed and solid lines correspond to the scenario when 2nd qubit and both qubits interact with the environment, respectively. The horizontal line denotes for the classical upper bound of the TF, $2/3$.

Scenario - I : In this scenario the 2nd qubit, during the transit, interacts with the environment while the 1st qubit has been isolated from the environment. After receiving the 2nd qubit by Bob, the shared state becomes

$$\begin{aligned} \rho_{12}^D &= U_{2,0}\rho_{12}U_{2,0}^\dagger + U_{2,1}\rho_{12}U_{2,1}^\dagger \\ &= \begin{pmatrix} \frac{1}{2} & 0 & 0 & \frac{\sqrt{D_2}}{2} \\ 0 & 0 & 0 & 0 \\ 0 & 0 & \frac{D_2}{2} & 0 \\ \frac{\sqrt{D_2}}{2} & 0 & 0 & \frac{D_2}{2} \end{pmatrix}, \end{aligned} \quad (9)$$

where $\rho_{12} = |\psi\rangle_{12}\langle\psi|$, $U_{2,0} = I \otimes W_{2,0}$ and $U_{2,1} = I \otimes W_{2,1}$. The concurrence and TF of the state ρ_{12}^D become

$$\begin{aligned} C(\rho_{12}^D) &= \sqrt{1 - D_2} \\ F(\rho_{12}^D) &= \frac{1}{6} \left(4 + 2\sqrt{1 - D_2} - D_2 \right), \end{aligned} \quad (10)$$

From Eq. (10), it can be shown that the state becomes separable, i.e., $C(\rho_{12}^D) = 0$ for $D = 1$, and TF drops to the classical region, i.e., $F \leq 2/3$ for $(2\sqrt{2} - 2) \leq D \leq 1$. Interestingly, although the state ρ_{12}^D is entangled for $(2\sqrt{2} - 2) \leq D < 1$, but it is not useful for teleportation. The dashed lines in the Figs. 1(a)-(b) correspond to the variation of concurrence $C(\rho_{12}^D)$ and TF $F(\rho_{12}^D)$ with respect to the strength of decoherence D_2 , respectively. Interestingly, the state ρ_{12}^D is not useful for teleportation although it is entangled in the range of strength of decoherence, $(2\sqrt{2} - 2) \leq D < 1$. The CC of the state ρ_{12}^D , $CC(\rho_{12}^D)$ has been calculated numerically and plotted (dashed line) in the Fig. 1(c). It shows that classical correlation decreases when D increases.

Scenario - II : When both qubits interact with the local environment, Alice and Bob share the following state

$$\begin{aligned} \rho_{12}^{DD} &= V_{1,0}\rho_{12}V_{1,0}^\dagger + V_{1,1}\rho_{12}V_{1,1}^\dagger, \\ &= \begin{pmatrix} \frac{1+D_1D_2}{2} & 0 & 0 & \frac{\sqrt{D_1D_2}}{2} \\ 0 & \frac{D_1D_2}{2} & 0 & 0 \\ 0 & 0 & \frac{D_1D_2}{2} & 0 \\ \frac{\sqrt{D_1D_2}}{2} & 0 & 0 & \frac{D_1D_2}{2} \end{pmatrix}, \end{aligned} \quad (11)$$

where $V_{1,0} = W_{1,0} \otimes I$ and $V_{1,1} = W_{1,1} \otimes I$. The concurrence and TF of the state ρ_{12}^{DD} become

$$\begin{aligned} C(\rho_{12}^{DD}) &= (1 - D)(\sqrt{1 + D^2} - D) \\ TF(\rho_{12}^{DD}) &= \frac{1}{3}(3 - 2D + D^2), \end{aligned} \quad (12)$$

where, for simplicity, $D_2 = D_1 = D$ has been considered. The CC has been calculated numerically and plotted (solid line) in the Fig. 1(c). The Fig. 1(a) shows that when decoherence acts on both qubits, the concurrence $C(\rho_{12}^{DD})$ drops more rapidly than the case of $C(\rho_{12}^D)$ when decoherence acts on a single qubit. Interestingly, the effect of decoherence on both qubits activates TF in the non-classical region for $2(\sqrt{2} - 1) \leq D < 1$ where the state ρ_{12}^D has TF in the classical region [31]. Therefore, decoherence can activate the non-classical information processing task, teleportation. In the Ref. [11], the author commented that, as in the teleportation, both quantum correlation (entanglement) and classical correlation play the role, and TF has been activated due to the contribution of the classical part of the correlation. The Fig. 1(c) shows that decoherence on both qubits enhances the classical correlation than decoherence acting on a single qubit. At $D = 1$, $C(\rho_{12}^{DD}) = 0$ and $CC(\rho_{12}^{DD}) = 1$, and therefore the maximum classical correlation corresponds to $TF = 2/3$. When $D \rightarrow 1$, non-vanishing entanglement ($C(\rho_{12}^{DD}) \neq 0$) and high classical correlation ($CC(\rho_{12}^{DD}) \rightarrow 1$) make TF in the non-classical region. This supports the comment of the Ref. [11].

V. OPTIMIZED PROTECTION OF ENTANGLEMENT AND TF IN THE PRESENCE OF DECOHERENCE USING THE TECHNIQUE OF WEAK MEASUREMENT AND ITS REVERSAL

In the WMRWM technique, to minimize the effect of ADC on the i th ($i \in \{1, 2\}$) qubit, a positive operator valued measurement (POVM, known as weak measure-

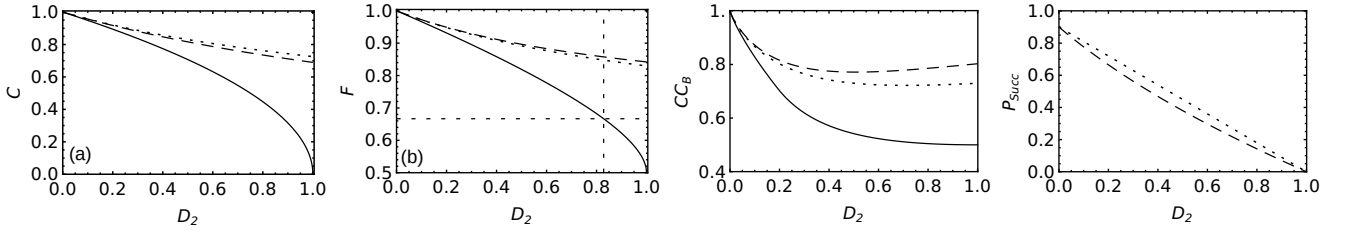


FIG. 2. Comparison of improvement of (a) entanglement, (b) teleportation fidelity, (c) classical correlation and (d) success probability of the state σ_{12}^R (of Eq. (16)) with respect to the strength of decoherence while considering the weak measurement strength $p_2 = 0.1$. The solid line corresponds to the case when the technique of WMRWM is not applied, i.e., for the state ρ_{12}^D of Eq. (9). The dashed and dotted lines represent the case when TF and concurrence is being maximized with respect to the strength of reverse weak measurement, respectively. The horizontal line denotes for the classical upper bound of the TF, $2/3$.

ment),

$$W_{i,0} = \begin{pmatrix} 1 & 0 \\ 0 & \sqrt{p_i} \end{pmatrix} \quad (13)$$

has been performed. Here, p_i is the strength of weak measurement. Weak measurement can be experimentally realized by reducing the sensitivity of the detector, i.e., the detector never clicks if the qubit is in the state $|0\rangle_i$ and clicks with probability p_i if the qubit is in the state $|1\rangle_i$ [27, 33–35]. Here, $W_{i,0}$ corresponds to the case when the detector does not click. Therefore, the weak measurement $W_{i,0}$ maps the initial state ρ_i towards $|0\rangle_i$ which remains unaffected by ADC. After decoherence acting on the respective systems, a reverse weak measurement,

$$R_{i,0} = \begin{pmatrix} \sqrt{q_i} & 0 \\ 0 & 1 \end{pmatrix} \quad (14)$$

has been performed on the i th qubit. Here, q_i is the strength of reverse weak measurement. Finally to protect quantum properties optimally, maximization is taken over the parameter q_i . Note that in the realization of weak measurement, the protocol fails when the detector clicks. Therefore, the technique of WMRWM is associated with success probability which corresponds to the failure to register the qubit by the detector. Similar to the Sec. IV, here, two different scenarios have been considered.

Scenario I : Here, decoherence acts on the 2nd qubit. To protect quantum features of the initial state $|\psi\rangle_{12}$ of Eq. (5), Alice makes weak measurement $W_{2,0}$ on the 2nd qubit with strength p_2 . As a result of weak measurement, Alice sends the following state to Bob,

$$\sigma_{12}^W = (I \otimes W_{2,0})\rho_{12}(I \otimes W_{2,0}^\dagger). \quad (15)$$

Then she sends the 2nd qubit to Bob. Due to environmental interaction the state becomes $\sigma_{12}^D = U_{2,0}\sigma_{12}^W U_{2,0}^\dagger + U_{2,1}\sigma_{12}^W U_{2,1}^\dagger$. After receiving the qubit, Bob makes reverse weak measurement $R_{2,0}$ with strength q_2 . Finally, Alice and Bob share the following state $(I \otimes R_{2,0})\sigma_{12}^D(I \otimes R_{2,0}^\dagger)$ with probability $P_\sigma^R = \text{Tr}[(I \otimes R_{2,0})\sigma_{12}^D(I \otimes R_{2,0}^\dagger)]$.

The normalized shared state becomes

$$\sigma_{12}^R = \frac{1}{P_\sigma^R} (I \otimes R_{2,0})\sigma_{12}^D(I \otimes R_{2,0}^\dagger) = \begin{pmatrix} \frac{\bar{q}_2}{\alpha} & 0 & 0 & \sqrt{D_2 \bar{p}_2 \bar{q}_2} \\ 0 & 0 & 0 & 0 \\ 0 & 0 & \frac{D_2 \bar{p}_2 \bar{q}_2}{\alpha} & 0 \\ \frac{\sqrt{D_2 \bar{p}_2 \bar{q}_2}}{\alpha} & 0 & 0 & \frac{D_2 \bar{p}_2}{\alpha} \end{pmatrix}, \quad (16)$$

where $\alpha = (2 - p_2 - q_2 - D_2 \bar{p}_2 \bar{q}_2)$. As the weak measurement and reverse weak measurement are associated with a success probability of not registering the incoming photon, the success probability of obtaining the state σ_{12}^R from initially prepared maximally entangled state becomes

$$P_{\text{Succ}} = \frac{\alpha}{2}. \quad (17)$$

The FEF and TF of the state σ_{12}^R are given by

$$f(\sigma_{12}^R) = \frac{\bar{p}_2 + \bar{q}_2 - D_2 \bar{p}_2 + 2\sqrt{D_2 \bar{p}_2 \bar{q}_2}}{2\alpha},$$

$$F(\sigma_{12}^R) = \frac{2f(\sigma_{12}^R) + 1}{3}, \quad (18)$$

and the concurrence becomes

$$C(\sigma_{12}^R) = \frac{2\sqrt{D_2 \bar{p}_2 \bar{q}_2}}{\alpha}. \quad (19)$$

Next, we study optimal preservation of $F(\sigma_{12}^R)$ and $C(\sigma_{12}^R)$ with respect to the strength of reverse weak measurement q_2 . It is interesting that *whether optimization of $F(\sigma_{12}^R)$ implies optimization of $C(\sigma_{12}^R)$* . It is also interesting that how the above mentioned optimizations affect the classical correlation of the state σ_{12}^R .

Optimized teleportation fidelity : To minimize the effect of ADC on teleportation, $F(\sigma_{12}^R)$ of Eq. (18) needs to be maximized with respect to q_2 . The maximum value of TF,

$$F^{\text{max}}(\sigma_{12}^R) = \frac{3 + 2 D_2 \bar{p}_2}{3 + 3 D_2 \bar{p}_2} \quad (20)$$

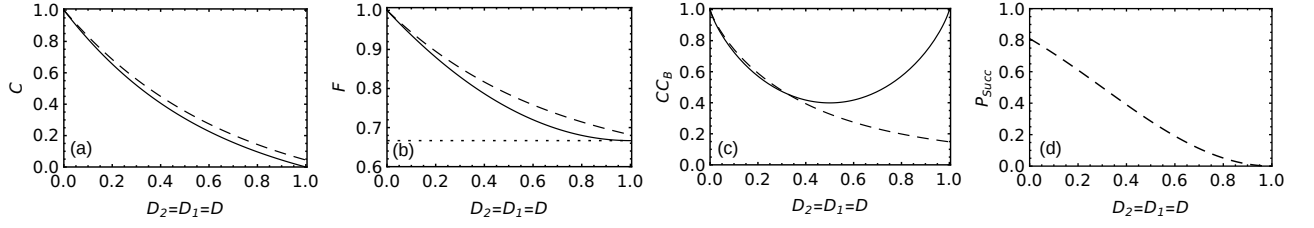


FIG. 3. Comparison of improvement of (a) entanglement, (b) teleportation fidelity, (c) classical correlation and (d) success probability of the state σ_{12}^R (of Eq. (28)) with respect to the strength of decoherence while considering the weak measurement strength $p_2 = 0.1$. The solid line corresponds to the case when the technique of WMRWM is not applied, i.e., for the state ρ_{12}^{DD} of Eq. (11). The dashed line represents the case when TF and C are maximized with respect to the strength of reverse weak measurement. The dotted horizontal line denotes for the classical upper bound $2/3$ of the TF.

occurs for the choice of strength of reverse weak measurement given by

$$q_2^{\max} = \frac{3D_2\bar{p}_2 + D_2^2\bar{p}_2^2 + p_2}{(1 + D_2\bar{p}_2)^2}. \quad (21)$$

For the above choice of q_2^{\max} , the concurrence of the state σ_{12}^R becomes

$$C^{q_2^{\max}}(\sigma_{12}^R) = \frac{2}{2 + D_2\bar{p}_2}, \quad (22)$$

and the $CC^{q_2^{\max}}(\sigma_{12}^R)$ is numerically calculated. The dashed line in the Fig. 2(c) shows the variation of CC for the choice of $p_2 = 0.1$. Here, the success probability becomes

$$P_{Succ}^{q_2^{\max}}(\sigma_{12}^R) = \frac{\bar{D}_2(2 + D_2\bar{p}_2)\bar{p}_2}{2 + 2D_2\bar{p}_2}. \quad (23)$$

Optimized concurrence : In this case, the concurrence of the state $F(\sigma_{12}^R)$ of Eq. (18) has been maximized with respect to the strength of reverse weak measurement q_2 . The maximum value of concurrence

$$C^{\max}(\sigma_{12}^R) = \frac{1}{\sqrt{1 + D_2\bar{p}_2}} \quad (24)$$

occurs for the

$$q_2^{\max} = \frac{p_2 + 2D_2\bar{p}_2}{1 + D_2\bar{p}_2}. \quad (25)$$

For the choice of q_2^{\max} , the TF becomes

$$F^{q_2^{\max}}(\sigma_{12}^R) = \frac{1}{6} \left(3 + 2 \frac{1}{\sqrt{1 + D_2\bar{p}_2}} + \frac{1}{1 + D_2\bar{p}_2} \right) \quad (26)$$

The dotted line in the Fig. 2(c) correspond to the CC for $p_2 = 0.1$ when concurrence has been maximized. In this case, the success probability becomes

$$P_{Succ}^{q_2^{\max}}(\sigma_{12}^R) = \bar{D}_2\bar{p}_2. \quad (27)$$

The above two optimization cases have been compared in the Fig. (2) with the *Scenario-I* of the Sec IV. Here, the solid line corresponds to the case when the

technique WMRWM has not been applied, dashed line represents the case when TF is maximized under the technique of WMRWM, and dotted line corresponds to the case when concurrence has been maximized for $p_2 = 0.1$. The Fig. 2(b) shows that When TF has been maximized with respect to the strength of reverse weak measurement, TF of the state σ_{12}^R gives slightly larger value than the case when concurrence is maximized. Similarly, in the Fig. 2(a), concurrence of the state σ_{12}^R is slightly larger when concurrence is maximized than TF. But, when the strength of weak measurement increases, the difference between both cases, i.e., TF-maximized and concurrence-maximized reduces, i.e., $F^{q_2^{\max}}(\sigma_{12}^R) \rightarrow F^{\max}(\sigma_{12}^R)$ and $C^{q_2^{\max}}(\sigma_{12}^R) \rightarrow C^{\max}(\sigma_{12}^R)$ for $p_2 \rightarrow 1$. Interestingly, the Fig. 2(c) shows that when TF is maximized, the classical correlation is also maximized. Therefore, the Fig. (2) justifies the comment in the conclusion of the Ref. [11]. The Fig. 2(d) represents the comparison of the success probability of these two cases. It shows that concurrence maximization has larger success probability than TF maximization for $0 < D < 1$.

Scenario II : Here, we have considered that the WM-RWM technique has been applied on both the qubits when both of them are affected by the ADC. Similar to the *Scenario I* (of this section), after preparing two qubits in the maximally entangled state of Eq. (5), Alice makes weak measurement. As a result the combined state becomes $\sigma_{12}^{WW} = (W_{1,0} \otimes W_{2,0})\rho_{12}(W_{1,0}^\dagger \otimes W_{2,0}^\dagger)$. Due to interaction with the environment, the shared state becomes $\sigma_{12}^{DD} = V_{1,0}\rho_{12}^{DWW}V_{1,0}^\dagger + V_{1,1}\rho_{12}^{DWW}V_{1,1}^\dagger$, where $\rho_{12}^{DWW} = U_{2,0}\sigma_{12}^{WW}U_{2,0}^\dagger + U_{2,1}\sigma_{12}^{WW}U_{2,1}^\dagger$. Next, both Alice and Bob make reverse weak measurement on their respective systems. The shared state becomes

$$\begin{aligned} \sigma_{12}^{RR} &= (R_{1,0} \otimes R_{2,0})\sigma_{12}^{DD}(R_{1,0} \otimes R_{2,0}^\dagger) \\ &= \begin{pmatrix} \frac{\bar{q}^2(1+D^2\bar{p}^2)}{\beta} & 0 & 0 & \frac{\bar{D}\bar{p}\bar{q}}{\beta} \\ 0 & \frac{D\bar{D}\bar{p}^2\bar{q}}{\beta} & 0 & 0 \\ 0 & 0 & \frac{D\bar{D}\bar{p}^2\bar{q}}{\beta} & 0 \\ \frac{\bar{D}\bar{p}\bar{q}}{\beta} & 0 & 0 & \frac{\bar{D}^2\bar{p}^2}{\beta} \end{pmatrix}, \quad (28) \end{aligned}$$

where $\beta = 2 - 2q(1 + D\bar{p}^2) + q^2(1 + D^2\bar{p}^2) - (2 - p)p$.

Here, for simplicity, $D_2 = D_1 = D$, $p_2 = p_1 = p$ and $q_2 = q_1 = q$ have been considered. Similar to the *Scenario-I* in the Sec. V, here, we have also considered two different cases - *optimized teleportation fidelity* and *optimized concurrence*. The success probability of getting the state σ_{12}^{RR} becomes

$$P_{\text{Succ}}(\sigma_{12}^{RR}) = \frac{\beta}{2} \quad (29)$$

For the shared state σ_{12}^{RR} , the FEF becomes

$$f(\sigma_{12}^{RR}) = \frac{D^2(1 + \bar{q}^2)\bar{p}^2 - 2D\bar{p}(\bar{p} + \bar{q}) + (\bar{p} + \bar{q})^2}{\beta} \quad (30)$$

and the concurrence is given below

$$C(\sigma_{12}^{RR}) = \frac{\bar{D}\bar{p}\bar{q}(\delta_1 - \delta_2 - 2D\bar{p})}{\beta}, \quad (31)$$

where $\delta_1 = \sqrt{2(1 + \sqrt{1 + D^2\bar{p}^2}) + D^2\bar{p}^2}$ and $\delta_2 = \sqrt{2(1 - \sqrt{1 + D^2\bar{p}^2}) + D^2\bar{p}^2}$.

Optimized teleportation fidelity : Maximizing $f(\sigma_{12}^{RR})$ with respect to q , the optimized TF becomes

$$F^{\text{max}}(\sigma_{12}^{RR}) = \frac{(2 + (1 - \eta)(\sqrt{1 + \eta^2} - \eta))}{3}, \quad (32)$$

where $\eta = D\bar{p}$ and the corresponding strength of reverse weak measurement is given by

$$q_{12}^{\text{max}} = \frac{\sqrt{1 + \eta^2} - \bar{p}\bar{D}}{\sqrt{1 + \eta^2}}. \quad (33)$$

The concurrence for the choice of q_{12}^{max} becomes

$$C^{q_{12}^{\text{max}}}(\sigma_{12}^{RR}) = \frac{1}{2} (\sqrt{1 + \eta^2} - \eta) (\delta_1 - \delta_2 - 2D\bar{p}) \quad (34)$$

In this case, the CC is calculated numerically and shown in the Fig. 3(c) with dashed line for the choice of $p_2 = 0.1$.

Optimized concurrence : Interestingly, in this case, the maximum value of concurrence occurs for the same strength of the reverse weak measurement q_{12}^{max} of Eq. (33). Therefore, the maximum value of concurrence becomes $C^{\text{max}}(\sigma_{12}^{RR}) = C^{q_{12}^{\text{max}}}(\sigma_{12}^{RR})$ and corresponding TF is of the form of $F^{\text{max}}(\sigma_{12}^{RR})$. Also, the CC become same in both the cases in this scenario.

Surprisingly, unlike the *Scenario-I* (in the Sec. V), in the present scenario, the $C^{\text{max}}(\sigma_{12}^{RR})$ becomes smaller than $C(\rho_{12}^{DD})$ for larger value of the strength of decoherence, i.e., $D > 0.33$. But the improvement of TF of the state σ_{12}^{RR} for larger values of D implies that classical correlation does not always help to improve the TF.

VI. CONCLUSION

In conclusion, in the present work, we have studied the behavior of TF, entanglement and CC in the presence of decoherence and protected them with the help of the technique of WMRWM. Comparing the scenarios where single and both qubits interact via ADC, TF has been activated (from the classical to non-classical region) in the second scenario for $(2\sqrt{2} - 2) < D < 1$. As both CC and entanglement take part in teleportation, in the second scenario, CC (which increases significantly) plays the key role over entanglement in teleportation. While decoherence decreases the entanglement, and it enhances the CC. This phenomenon also holds in the case where WMRWM is applied only on the 2nd qubit. In this scenario, interestingly, maximization of TF does not maximize concurrence. CC has a larger value when TF has been maximized. When WMRWM is applied on both qubits, the improvement of TF occurs due to the improvement of concurrence. It will be interesting to explore the roles of classical correlation and entanglement to obtain non-classical teleportation fidelity.

VII. ACKNOWLEDGEMENTS

The author thanks Tanumoy Pramanik for the discussion and helpful comments.

-
- [1] M. A. Nielsen and I. L. Chuang, *Quantum computation and quantum information* (Cambridge University Press, 2000)
 - [2] R. Horodecki, P. Horodecki, M. Horodecki, and K. Horodecki, *Rev. Mod. Phys.* **81**, 865 (2009).
 - [3] C.H. Bennett, G. Brassard, C. Crépeau, R. Jozsa, A. Peres, and W.K. Wootters, *Phys. Rev. Lett.* **70** 1895 (1993).
 - [4] D. Bouwmeester, J.-W. Pan, K. Mattle, M. Eibl, H. Weinfurter, and A. Zeilinger, *Nature* **390**, 575 (1997).
 - [5] D. Boschi, S. Branca, F. De Martini, L. Hardy, and S. Popescu, *Phys. Rev. Lett.* **80**, 1121 (1998).
 - [6] I. Marcikic, H. de Riedmatten, W. Tittel, H. Zbinden, and N. Gisin, *Nature* **421**, 509 (2003).
 - [7] Ji-Gang Ren et al., *Nature* **549**, **70** (2017).
 - [8] A. Peres, W.K. Wootters, *Phys. Rev. Lett.* **66** 1119 (1991).
 - [9] S. Massar, S. Popescu, *Phys. Rev. Lett.* **74** 1259 (1995).
 - [10] M. Horodecki, P. Horodecki, R. Horodecki, *Phys. Rev. A* **60** 1888 (1999).
 - [11] S. Bandyopadhyay, *Phys. Rev. A* **65** 022302 (2002).
 - [12] L. Henderson, and V. Vedral, *J. Phys. A: Math. Gen.* **34** 6899 (2001).

- [13] H. Ollivier, and W. H. Zurek, Phys. Rev. Lett. **88** 017901 (2001).
- [14] W.K. Wootters, Phys. Rev. Lett. **80**, 2245 (1998).
- [15] M. Horodecki, P. Horodecki, and R. Horodecki, Phys. Rev. A **60**, 1888 (1999).
- [16] S. Albeverio, S.M. Fei, and W. L. Yang, Phys. Rev. A, **66**, 012301(2002).
- [17] F. Verstraete, H. Verschelde, Phys. Rev. A **66**, 022307 (2002).
- [18] S. Adhikari, A. S. Majumdar, S. Roy, B. Ghosh, and N. Nayak, Quant. Inf. Compt. **10**, 0398 (2010).
- [19] T. Yu and J. H. Eberly, Science **323**, 598 (2009).
- [20] A. Salles, F. de Melo, M. P. Almeida, M. Hor-Meyll, S. P. Walborn, P. H. Souto Ribeiro, and L. Davidovich, Phys. Rev. A **78**, 022322 (2008).
- [21] R. Chaves, D. Cavalcanti, L. Aolita, and A. Acín, Phys. Rev. A **86**, 012108 (2012).
- [22] M. P. Almeida, F. de Melo, M. Hor-Meyll, A. Salles, S. P. Walborn, P. H. Souto Ribeiro, L. Davidovich, Science **316**, 579 (2007).
- [23] T. Pramanik, Y.-W. Cho, S.-W. Han, S.-Y. Lee, S. Moon, and Y.-S. Kim, Phys. Rev. A **100**, 042311 (2019).
- [24] H.-T. Lim, K.-H. Hong, and Y.-H. Kim, Sci. Rep. **5**, 15384 (2015).
- [25] S. Oh, S. Lee, and H.-W. Lee, Phys. Rev. A **66**, 022316 (2002).
- [26] H. Prakash, N. Chandra, R. Prakash, and Shivani, J. Phys. B: At. Mol. Opt. Phys. **40** 1613 (2007).
- [27] T. Pramanik, A.S. Majumdar, Phys. Lett. A **377** 3209 (2013).
- [28] M.B. Plenio, S.F. Huelga, Phys. Rev. Lett. **88** 197901 (2002).
- [29] D. Braun, Phys. Rev. Lett. **89** 277901 (2002);
- [30] M. S. Kim, Jinhyoung Lee, D. Ahn, and P. L. Knight, Phys. Rev. A **65** 040101(R) (2002).
- [31] P. Badziag, M. Horodecki, P. Horodecki, R. Horodecki, Phys. Rev. A **62** 012311 (2000).
- [32] M. Koashi, M. Ueda, Phys. Rev. Lett. **82** 2598 (1999).
- [33] Y.-S. Kim, Y.-W. Cho, Y.-S. Ra, Y.-H. Kim, Opt. Express **17** 11978 (2009).
- [34] J.-C. Lee, Y.-C. Jeong, Y.-S. Kim, Y.-H. Kim, Opt. Express **19** 16309 (2011).
- [35] Y.-S. Kim, J.-C. Lee, O. Kwon, Y.-H. Kim, Nat. Phys. **8** 117 (2012).
- [36] S. Popescu, Phys. Rev. Lett. **74**, 2619 (1995).
- [37] M. B. Plenio, S. F. Huelga, A. Beige, and P. L. Knight, Phys. Rev. A **59**, 2468 (1999).
- [38] M. Navascúes, and T. Vertesi, Phys. Rev. Lett. **106**, 060403 (2011).
- [39] T. Pramanik, Y.-W. Cho, S.-W. Han, S.-Y. Lee, Y.-S. Kim, and S. Moon, Phys. Rev. A **99**, 030101(R) (2019).
- [40] T. Yu and J. H. Eberly, Science **323**, 598 (2009).
- [41] A. Salles, F. de Melo, M. P. Almeida, M. Hor-Meyll, S. P. Walborn, P. H. Souto Ribeiro, and L. Davidovich, Phys. Rev. A **78**, 022322 (2008).
- [42] M. P. Almeida, F. de Melo, M. Hor-Meyll, A. Salles, S. P. Walborn, P. H. Souto Ribeiro, L. Davidovich, Science **316**, 579 (2007).
- [43] T. Pramanik, Y.-W. Cho, S.-W. Han, S.-Y. Lee, S. Moon, and Y.-S. Kim, Phys. Rev. A **100**, 042311 (2019).
- [44] D. Cavalcanti, P. Skrzypczyk, and I. Šupić, Phys. Rev. Lett. **119**, 110501 (2017).
- [45] C.H. Bennett, D.P. Di Vincenzo, J.A. Smolin, and W.K. Wootters, Phys. Rev. A **54** 3824 (1996).
- [25] A. Sohbi, I. Zaquine, E. Diamanti, and D. Markham, Phys. Rev. A **91**, 022101 (2015).